I.A.U
Karaj branch

Journal of
A p p l ied
C hemical
R esearch
jacr.kiau.ac.ir

Journal of Applied Chemical Research, 17, 4, 46-62 (2023)

Investigation of the Drug Delivery Potential of a Transdermal Patch Based on Buprenorphine Templated Molecular Imprinted Polymer

Nasrin Behnia[1], Parviz Aberoomand Azar[*1], Maryam Shekarchi*[2,3], Mohammad Saber Tehrani[1], Noushin Adib[2]

[1]*Department of Chemistry, Science and Research Branch, Islamic Azad University, Tehran, Iran*

[2]*Food and Drug Laboratory Research Centre, Food and Drug Organization, MOH&ME, Tehran, Iran*

[3]*Pharmaceutical Research Center, Tehran University of Medical Science, Tehran, Iran*

(Received 22 Feb. 2023; Final revised received 10 May 2023)

Abstract

To synthesize the molecular imprinted polymer (MIP), the well-known precipitation polymerization method was used. To do this, Methacrylic acid (MAA; as the functional monomer), ethylene glycol dimethacrylate (EGDMA; as the cross-linker), and 2,2-azobisissobutyronitrile (AIBN; as the initiator), were used. In addition, to control the release rate of Buprenorphine (BUP) from the patch, the bacterial cellulose (BC) was applied. The release process of the drug was investigated by high performance liquid chromatography (HPLC) system, which was showed to be fitted with the Higuchi expression. Moreover, the results have indicated that the obtained MIP-BC is a suitable candidate for the control released transdermal drug delivery. The work revealed that using MIP is more suitable compared to non-imprinted polymer (NIP). In addition, those results indicated that the MIP could be used as a patch for drug delivery application at least in the case of BUP drug.

Keywords: Molecular imprinted polymer, Buprenorphine, Bacterial cellulose, Transdermal patch, Drug delivery.

[*]***Corresponding authors:*** *Parviz Aberoomand Azar, Maryam Shekarchi, Department of Chemistry, Science and Research Branch, Islamic Azad University, Tehran, Iran. Food and Drug Laboratory Research Center, Food and Drug Organization, MOH & ME, Tehran, Iran. Emails: parvizaberoomand@gmail.com, Shekarchim@yahoo.com.*

Introduction

Buprenorphine (BUP) is one of the most important opioids, which is able to relieve severe pains like the cancer related ailments. Several BUP formulations containing the controlled-release tablets, as well as the liquid forms have been commercially introduced due to the wide usage of this drug [1]. Optimization of the release rate of the medicines into the blood has always been crucial for experts. It was more important when the bioavailability (and the release rate) of a drug was higher; while, the shelf life of that and the dosage required for body was lower [2]. Several approaches for optimization of the release rate of the medicines such as the osmotic pumps [3], the slow-release tablets [4], the molecular imprinted polymers (MIPs) [5], and the sol-gels were designed for BUP[6].

The molecular imprinting technology (MIT), has recently been developed to resolve a wide range of problems in different area. The MIPs, which are of the best achievements of this technology, have been considered as a key candidate for drug delivery systems [7]. In such systems, polymers are obtained in presence of a medicinal compound as molecular template (Figure 1). When the polymer was synthesized, the it was washed for several times to make that free of those template molecules. Thus, the polymer matrix would be full of free receptor positions, which could receive the drug for further use [8]. It is clear that such valuable hosts could be applied as the stationary phase for the chromatography columns packing [9], nano sized actuators [10], nano sorbents [11], biosensors [12], and new tiny drug release systems [13].

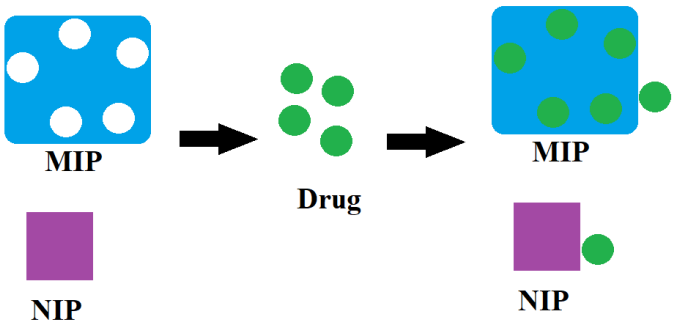

Figure 1. The absorption process of BUP by MIP host compared to NIP as reference.

With the aid of the MIP technology, formulators could obtain certain dosages and regulate the release rates of the drugs [14] which could be considered as a key advantage of such technique. In addition, the transdermal drug delivery (TDD) system is a new painless approach that has recently been taken into further considerations. The TDD system has numerous benefits compared to some of the other drug delivery methods. The first benefit of

this system is the elimination of the hepatic first-pass metabolism and the changes in the metabolic components and in the bioavailability of the molecules which are caused by cytochrome enzymatic proteins [15]. The second advantage of it, is protecting the drug compounds from the acidic environment of the digestive system [16]. In addition, the third one, is its controllable release rate. Moreover, this approach is painless. Somehow, it could release the drug for a long period of time (up to a week). Also, the required dosage of the drug is lower and the treatment is less expensive. However, this method could be applied for a limited range of drugs.

Thus, we have applied BUP compound as the molecular template for obtaining the MIP granules for application in the TDD system. The membrane of the bacterial cellulose was introduced to MIP and to NIP granules to obtain the cellulose modified MIP, and NIP, respectively. The scanning electron microscopy (SEM) was applied for morphology investigation and studying the cross section of transdermal patches. The drug release behavior of the composites and the ability of those for in vitro release was studied by high-performance liquid chromatography (HPLC) [17] applying a *Franz diffusion cell* [18,19]. The main goal of this project was to evaluate the drug release properties of MIP by applying types of kinetic models and to determine its related mechanism. The results of the work showed that using the MIP is more suitable compared to NIP. In addition, those results indicated that the MIP could be used as a device for drug delivery application (at least in the case of BUP compound).

Experimental

Materials and reagents

All of the chemicals and reagents and solvents were analytical grade. The ultra-pure water was obtained by a Milli-Q purification system (Millipore, Bedford, MA, USA). The compounds as well as the reagents containing 2,2-azobisissobutyronitrile (AIBN), methacrylic acid (MAA), N-Methylmorpholine N-oxide (NMMO), ethylene glycol dimethacrylate (EGDMA, 98% purity), N,N-dimethyl formamide (DMF), and polycaprolactone-triol (PCL-T), were prepared from Sigma-Aldrich company. In addition, monobasic potassium phosphate (KH_2PO_4) and acetonitrile were obtained from the Merck Chemicals. Also, the bacterial cellulose (BC), and BUP active pharmaceutical ingredient (API) were obtained from other commercial sources, accordingly.

Instrumentation

The Shimadzu Prominence HPLC system (Shimadzu Corporation, Kyoto, Japan) equipped with a DGU-20A degassing agent, a LC-20AD pump, a CTO-20A column oven and an SPD-20A UV-Vis detector, were applied for the required analyses. In addition, the Lab-Solutions software version 5.51 was applied for the data analysis and the required processing. Also, a C18, end-capped (250×4.6) mm, 5µm liquid chromatography column was used for the assaying analysis of the concentration of BUP. Moreover, a Spectrum 100 FT-IR spectrometer (PerkinElmer Co., Ltd., USA); a CR3i centrifuge (Thermo Fisher Scientific Inc., USA); a CHZ-82 constant temperature water bath oscillator (Fuhua Instrument Co. Lid., China); a FEI Quanta 200 scanning electron microscope (Thermo Fisher Scientific, Netherland); a KQ2200B sonic device with frequency and temperature controller (Kunshan Ultrosonic Instrument Co., Ltd., China) were used for the required tasks. Finally, a ZRS-8G dissolution tester (Tianda Tianfa Technology Co., Ltd., China) was applied for the release experiments.

Preparation of MIPs

Both of the MIPs and NIPs (as the reference) were obtained by the precipitation polymerization approach, and the UV photo polymerization, respectively. At the first step, 1 mmol of BUP was dissolved in 75 ml of DMF. Then, 4 mmol MAA, 20 mmol of EGDMA, and 50 mmol of AIBN were added to the mixture. Next, those were placed under ultrasonic waves for 10 min. Then, the mixture was purged by nitrogen atmosphere for 10 min [7-9]. Next, it was placed under UV irradiation at 366 nm for about one day. Finally, both of the MIP, and NIP were dried and grinned well for further use.

The prepared granules were powdered by grinding with a suitable mortar. Also, it should be noted that, the NIP (as reference) was synthesized under identical conditions without the presence of BUP as template. The schematic procedure for obtaining the MIP-BC has been presented in Figure 1.

Preparation of MIP-BC composite membrane

A 24 mg of the dried BC membrane was weighed accurately and was then held in 1.25 ml 50% aqueous NMMO at 60 ◦C for 60 minutes. The suspension was subsequently heated at 80 ◦C until a viscous, clear brown mixture of BC solution was prepared. Then, various portions of MIPs (containing 20, 30, 50 mg, respectively) and 75µl PCL-T as plasticizer were added to the suspension. Then, the suspension was poured into the mold (15 mm in diameter) until

the composite was formed by drying. Finally, the powder was grinded by a mortar for about 15 minutes to give a nano-sized composite with average particle sizes lower than 100 nm.

Characterization of the MIP-BC composite

SEM analysis

The surface morphology of the membranes was studies with the SEM which its photographs were obtained with a FEI ESEM QUANTA 200(USA). The cross-sections and surfaces of the initial cellulose, cellulose composite - MIPs and NIPs membranes were prepared by conductive deposition of the gold layer on the samples in a vacuum chamber. Figure 2 shows a SEM image of the membranes. In addition, the morphology of the samples was recorded under SEM scanning at the voltage of 25 kV, respectively.

FT-IR analysis

The FT-IR spectra of the NIP (as reference) and the MIP-BC were obtained by FT-IR analyzer. To reach this goal, a certain portion (about 5 mg) of the NIP-BC and the MIP-BC powders along with a 100 mg powder of KBr were mixed and grind well. Next, the mixture of the powders was pressed into a 1 mm pellet. The obtained samples were measured respectively on a Spectrum 100 FT-IR spectrometer. The FT-IR spectra of the NIP-BC and the MIP-BC were plotted by recording from 4000 to 400 cm^{-1} with a resolution of 2 cm^{-1} applying a pellet of KBr as the blank.

Friability of membranes

The physical strength of the membranes was assessed by Friability test. The membranes of MIPs and NIPs powders were rotated with friability device (Eraweka Abrasion Tester) with a speed of 25 rpm for 30 min. The friability of membrane was reached as the percentage of weight loss by following Equation:

$$\text{friability } (as\ dryness) = \frac{(Wi - Wf)}{Wi} * 100 \quad \text{Equation (1)}$$

According to the formula, W_i and W_f is the initial and the final weight of membranes.

Moisture Absorption

Before beginning the analysis, both of the NIP (as reference), and the MIP membranes were dried for three days at room temperature. Then, in order to evaluate the swelling capacity of

the membranes, those were weighed and were then placed in a buffer at pH 7.4 for 6 hours at room temperature. Next, the membranes were replaced and before weighing, the surfaces of composites were completely dried. The degree of swelling of the composites was reached, via Equation 2:

$$\text{Moisture Absorption} = \left(\frac{(W2-W1)}{W1}\right)*100 \quad \text{Equation (2)}$$

Where, W_1, W_2 are the MIP-BC weights before, and after the swelling processes, respectively.

Data analysis

In order to study the BUP transportation mechanism by the patches, three diffusion models containing the zero and the first orders as well as the Higuchi model were applied. The kinetic surveys were done by plotting the cumulative values of the drug (in percents) per time (in hours). The correlation coefficient (r) for each kinetic pattern was obtained to determine the model that was fitted:

The zero order model (concentration per time)

$Q = Q_0 + K_0 t$ Equation (3)

Higuchi's model (concentration per square root of time);

$Q_t/Q_0 = K_H\, t^{1/2}$ Equation (4)

First order pattern (logarithm of the concentration per time);

$\text{Log } Q_t = \log Q\, K_t$ Equation (5)

Where Q_t is amount diffused (mg) per time t (h), Q_0 is initial amount in donor compartment (µg). K_0 is the zero-order constant (µg h^{-1}), K_1 is first order constant (µg h^{-1}), and K_H is Higuchi's constant (µg $h^{1/2}$). The correlation coefficient (r) for each kinetic model was obtained to determine the fitted model.

Adsorption experiments

For the adsorption experiment, a 30.0 mg of the MIP-BC or the NIP-BC were suspended in 2 ml of phosphate buffer and a 10.0 mL of BUP solution (50 mg/L) at a different range of pHs for a time period between 2min – 240 min. Next, the sample solutions were filtered by a micro membrane, and the amount of the drug in filtrate was calculated by HPLC according to the procedure describe in the HPLC section. The binding capacity of the NIP as well as the MIP and the selectivity factor were obtained by Equations (6) and (7), respectively.

$Qt = (C_0-C_t)V/m$ Equation (6)

$\alpha = Q_{MIP}/Q_{NIP}$ Equation (7)

where Q_t (µmol/g) is the adsorption capacity in different times, C_0 (mmol/L) is the initial concentration of BUP, the Ct (mmol/L) is the concentration of BUP at the time t, V (in Liter) is the volume of the initial BUP solution, and m is the mass of the NIP-BC or the MIP-BC (in g). Finally, α is the selectivity factor of the NIP-BC to the MIP-BC, Q_{NIP} (µmol/g) is the adsorption capacity of the NIP, and Q_{MIP} (µmol/g) is the adsorption capacity of the MIP-BC.

release experiments

The process of the membrane penetration was performed by franz cell with a 0.95 cm^2 and a receptor chamber of a 5 mL volume. The release experiment was performed at 37 ± 1 °C in pH 7.4 potassium phosphate buffer (at the optimum pH), which had been stirred at a rate of 250 rpm by applying a magnetic stirrer. In addition, the release of BUP was determined by using the HPLC method. The cumulative release rate of BUP was calculated and plotted per time (2-240 min) Flux (J, $\mu g cm^{-2} min^{-1}$) was defined.

$$J = \frac{Q}{A*t}$$ Equation (8)

Where, the Q(µg) is the amount of analyte permeated, A(cm^2)is the effective membrane area and t (h) is the time.

HPLC method

The chromatographic determination of the concentration and release rate of BUP were carried out by a Shimadzu HPLC system occupied with a UV/VIS detector set at 220 nm. The LC separation was carried out by a C18 (4.6 mm, 250 mm, 5 µm) liquid chromatography column. The injection volume was 20 µL, the flow rate was 1 ml/min and the column temperature was fixed at 25°C by using the column oven. An isocratic method was used for the elusion and the mobile-phase was ACN/buffer solution with a 40/60, v/v percentage. Where, the buffer was prepared by dissolving the 10 mM of monobasic potassium phosphate in 1 liter of purified water set at pH of 2.5 by phosphoric acid [20-22].

Results and discussion

Structural characterization of the MIP-BC

FT-IR spectroscopic analysis

The FT-IR spectra of the BUP drug free-MIP-BC, and the BUP loaded MIP-BC, were shown in Table 1. The BUP drug free-MIP-BC represented strong absorption peaks at *v*C=O (stretching)=1729 cm^{-1}, *v*C-O (stretching)=1259 cm^{-1}, and *v*O-H (stretching)= 3436 cm^{-1}, due to OH bonds, as well as carboxyl groups from the MAA (functional monomer), and EGDMA (cross-linking agent).

By comparison, after loading the BUP molecule on the MIP-BC, the absorption peaks of C=O, C-O, and O-H, peaks, shifted to 1733 cm^{-1}, 1258 cm^{-1}, and 3424 cm^{-1}, respectively. On the other hand, the absorption peak of the O-H bond was increased and strengthened at 3434 cm^{-1} in the BUP loaded MIP-BC, which revealed about the formation of a hydrogen bond between BUP and the MIP.

Table 1. The wavelengths of the FT-IR spectra of MIP (A; black numbers), BUP-drug loaded MIP (B; blue numbers).

Wave number	**Wave length of Compound (cm-1)**	
	Drug-Free MIP	**BUP-drug loaded MIP**
1	3426.86	3550.42
2	2990.22	3437.62
3	2956.09	2989.36
4	1731.55	2955.08
5	1668.31	1731.41
6	1457.26	1669.3
7	1391.79	1458.81
8	1259.88	1390.72
9	1161.25	1257.65
10	960.52	1158.68
11	758.24	960.21
12	615.09	876.5
13	526.21	757.75
14		662.51

Physiochemical properties of MIP-BC composite

The results of swelling tests showed that the amount of this parameter (in percentage) for MIP-BC (containing 20 mg MIP+BC) is about 54.38%; while, its amount for NIP (containing 20 mg NIP+BC) is only about 40.76%.

Morphological structure analysis

As given in Figure 2, the surface of both the NIP, and MIP particles are probed by applying the SEM photographs. These figures indicate that both NIP and MIP particles have spherical morphologies and almost uniform structures. Also, the results confirmed that the average particle size is lower than 100 nm, both for NIP, and MIP, respectively. Indeed, the SEM images represented here indicate the uniform and regular texture of the nanocomposite. These also confirm that NIPs and MIPs, are in nano dimensions, due to their nano scale diameters. In addition, there is no considerable difference in the surface morphology between the MIP, and NIP. Thus, loading the BUP on the polymer or using it as the molecular template in the synthesis of MIP did not cause a considerable change on its surface morphology of the particles. Also, the oligomerization of the composite has been observed in some parts of the images. Such happening might be the result of the tendency for oligomerization and the increase in surface reactivity in the nano scale processing.

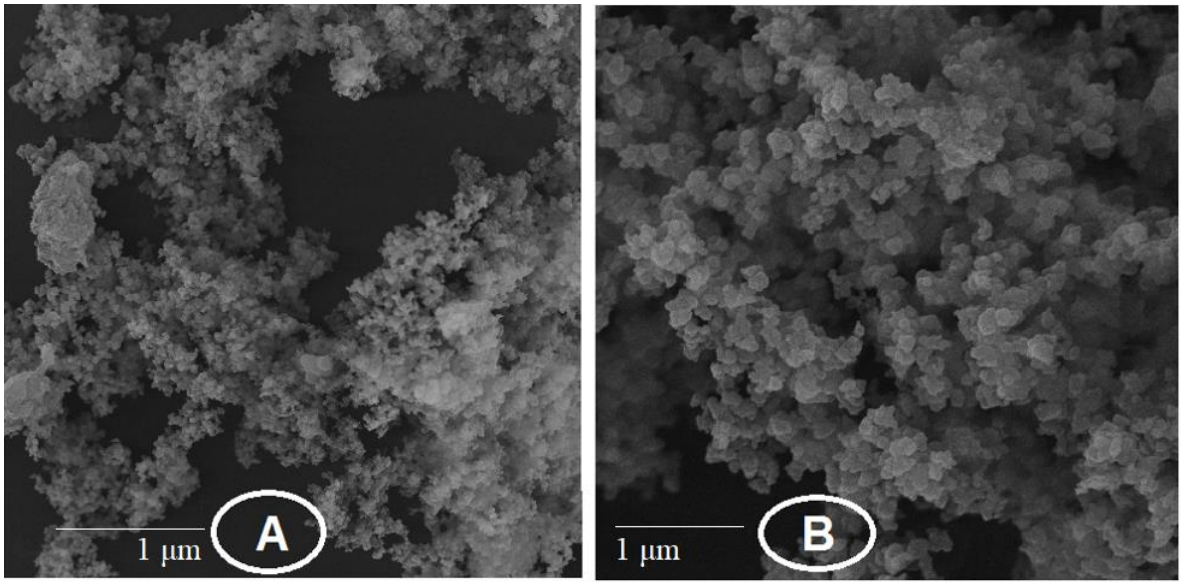

Figure 2. The SEM images of NIP nano particles (A), and MIP nano particles (B).

Adsorption behaviors of MIP-BC

Adsorption kinetics

The drug-adsorption behavior is one of the most important factors in the efficiency of the drug delivery systems. Usually, the pH value in solutions has a significant effect on drug adsorption and release processes. Thus, to inquire into the effect of pH on the drug absorption behavior of BUP in the case of the drug-loaded MIPs, the experiments were performed in a

pH range from 2.0 to 9.0. The relationship between the curves of the percentages of the cumulative adsorption in different pHs were presented in Table 2, Figure 3. The data of the profiles showed that the absorption percentage increases with the increasing pH up to 7.0. Moreover, it was shown that the ability of the MIP for adsorption of the BUP was significantly higher than that of NIP. It would be described as follows: the initial absorption was due to the physical adsorption as well as the non-specific binding (especially without hydrogen bonding) sites on the NIP surface. Also, the more efficient adsorption was controlled by the specific binding sites which was occurred by the imprinted sites.

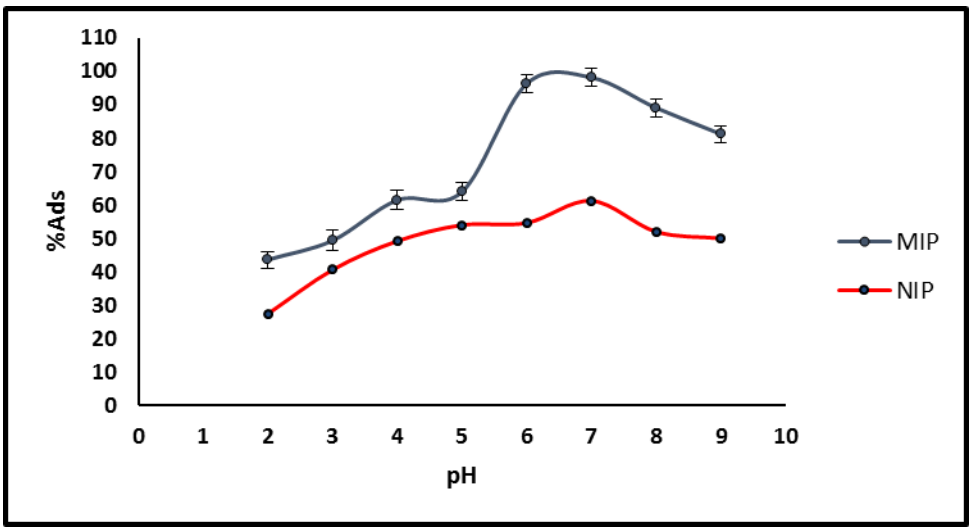

Figure 3. The curve of the changes of the adsorption of BUP by sorbents as a function of the changes of pHs.

The diagram of Figure 3 indicates that the cumulative adsorption rate (in %) at pH 7.0 was clearly higher than that at pH 2.0 – 5.0 and 8.0 to 9.0, proposing that the higher acidity of the environment would increase the drug desorption (perhaps due to protonation of the hydrogen acceptor cites (like the oxygen and nitrogen atoms)). It could lead to prevention of hydrogen bond formations. While, at pH 7.0, the loading of drug on the MIP has the highest cumulative amounts (%) due to weaker protonation in the neutral environment (and the stability of hydrogen bonds). Therefore, the performance of the drug absorption of the MIP is controlled by the pH values. Also, the lower release rate and stability at a higher pHs, indicate that the loaded-drug MIP-BC could be retained for a relatively longer time in the solution as well as in the blood plasma without a significant adverse effect on the tissue.

Table 2. Optimization of the adsorption of BUP both for NIP-BC, and MIP-BC at different pHs.

pH (n=3)	q_e (mg/g)- NIP	Adsorption (%)-NIP	q_e (mg/g)- MIP	Adsorption (%)-MIP
2	4.57	27.40	7.27	43.62
3	6.77	40.62	8.23	49.36
4	8.20	49.21	10.24	61.46
5	9.01	54.00	10.66	63.94
6	9.11	54.64	16.06	96.34
7	10.21	61.28	16.36	98.17
8	8.67	52.03	14.85	89.10
9	8.33	50.01	13.54	81.26

As shown in Table 1, the highest absorption amount is at pH=7.0 by the MIP (98.17%); while at the same condition (as the highest amount), the absorption of the drug by NIP is about 61.28%. It shows the priority of MIP for absorption of the BUP, compared to the NIP. On the other mean, the lowest absorption amounts belong to NIP (about 27.40%), and MIP (about 43.62 %) at pH=2, respectively. The other important note is that the change of the absorption percentage in the case of MIP is more depended on the change of the pH, compared to the NIP. It is another evidence for intervention of hydrogen bond formation in absorption of BUP by the MIP.

Drug release of composite

The controlled drug release of MIP contained tablets

Different ratios of MIP with cellulose were formulated as the receptor medium of the Franz diffusion cell. Different amounts of 20, 30, 40 and 50 mg of MIPs (Table 2) were composed with cellulose to make the patches. In addition, the membranes were clamped between the donor and the receptor sections containing phosphate buffer of pH 7.4 which is the pH of the human blood serum. The BUP release from the membrane with 50 mg of MIPs at first 30 min was 21.88%, at the first hour was 35.21, at 2 h was 48.76% and at 5h was 64.08%. Also, for a better understanding of the controlled release process of BUP (from the MIP), a control released tablet was made with the BUP-loaded MIP and BC (as excipients) for further release experiments.

Various kinetic curves were plotted to find the more reliable kinetic model and the best linearity was detected in Higuchi's pattern. Figure 4, shows the released process of BUP which following a Higuchi kinetic. Therefore, it has been shown that the release of BUP from

the matrix as a square root of time dependents on process based on Fickian diffusion which could be explained by the physicochemical properties of BUP as a polar compound that absorbs water, forming liquid crystalline mesophases. Such forms are able to control the drug release. As mentioned before, one of the key parameters in the efficiency of a drug delivery system is its drug-release behavior. Thus, to mimic the real conditions of the human body, and an accurate investigation on the release behavior of BUP in the drug-loaded MIPs, the absorption tests were performed in the pH=7.4 (which is the pH of the human blood serum [23,24]. Also, results of the pH optimization of the drug adsorption section) under continuous stirring at 37 ± 0.5 ◦C (the human body's normal temperature) was shown to be the best at pH=7.

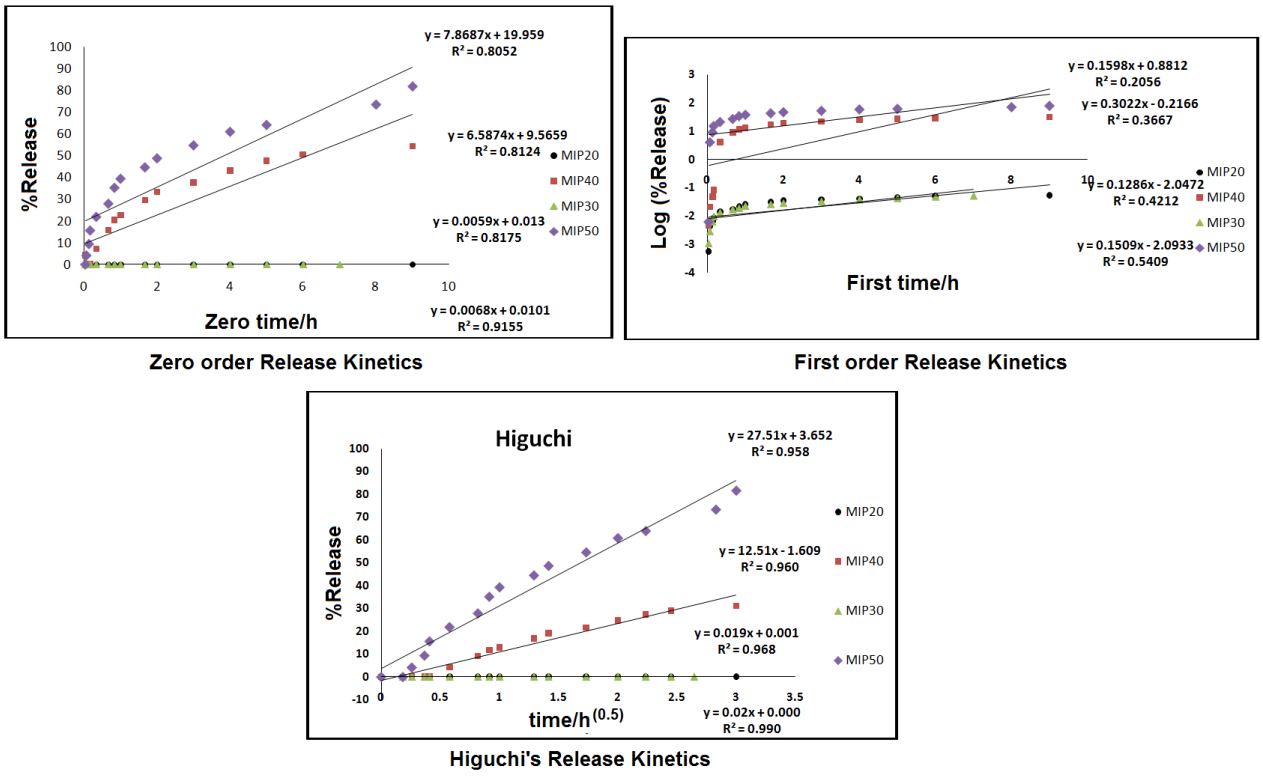

Figure 4. The Zero order, the first-order, and the Higuchi release kinetic model plots for various formulations of the BUP loaded MIP-BC nano-composites.

The relationship between the curves of the percentages of the cumulative release rate per time in different sorbents, were presented in Figure 4. The drug release data showed that the release rate rapidly increases along with the increase of time at first 60 min. While, the growth slows down at about the first 110 min. This process could be described as follows: the initial release was due to the physical adsorption with non-specific binding (especially

without any hydrogen bonding) substrates on the sorbent surface (which mostly occurs in the case of NIP as sorbent). In addition, the late (second) slow release was controlled by the specific binding sites (mostly occurs in the case of MIP). By comparison, the cumulative release rates (by percentage) were clearly lower in the case of MIP-BC, MIP, and NIP, respectively, which show that there are larger number of hydrogen bonds leading to a better control on the release rate of the drug (especially in case of imprinting sits).

Thus, at the above-mentioned conditions, the drug loaded MIP-BC had the lowest cumulative release rate (%) due to the higher number of hydrogen bonds between the BUP compound, and the imprinted receptors of the sorbent. It indicates that the performance of the BUP drug release by the MIP was mainly controlled by its formulation with the BC. Finally, the stability and the lower release rates at higher pHs, showed that the loaded-drug MIP could be retained for a longer time in the solution as well as in the blood serum without significant adverse effects on the tissues.

Table 3. R^2 value of Release Kinetic models of membranes.

Formulation Code	**Zero order(R^2)**	**First order(R^2)**	**Higuchi model(R^2)**
M_1 (20mg MIP)	0.9155	0.2056	0.9909
M_2 (30mg MIP)	0.8175	0.3667	0.9685
M_3 (40mg MIP)	0.8124	0.2166	0.9603
M_4 (50mg MIP)	0.8052	0.2056	0.9582

As shown in Figure 4 and Table 3, the R^2 value of the Zero-order, the first-order, and the Higuchi release kinetic models indicated that the release kinetic follows the Higuchi's pattern (R^2=0.9909 for M1, as the best formulation code). Since, the release kinetics was fitted with the Higuchi's pattern, the release process of the BUP seems to be controlled by the penetration of solute into the matrix (like diffusion release model).

Conclusions

The main advantage of using the MIP instead of some order previous methods like the usual tablets is the high adsorption-release percentage of each especial drug by its composite. One of the other advantages of using this composite is its selectivity to the templated drug. Also, the low cost and easy preparation are of the other benefits of applying this method.

One of the disadvantages of this method is its high sensitivity to the changes of pH values. Somehow, little changes on the pH of the solution directly effect on the adsorption-desorption

percentage of the drug by the MIP. Moreover, the in vivo use of MIP in the human blood vessels is difficult due to the problems in technology and real experiments.

Finally, it is suggested that in future, researchers perform in vivo experiments to investigate the effectiveness of this transdermal patch on the laboratory animals.

List of Abbreviations

2,2-azobisissobutyronitrile (AIBN)

Active pharmaceutical ingredient (API)

Bacterial cellulose (BC)

Buprenorphine (BUP)

Ethylene glycol dimethacrylate (EGDMA)

Fourier transform infrared (FTIR)

High performance liquid chromatography (HPLC)

Monobasic potassium phosphate (KH_2PO_4)

Methacrylic acid (MAA)

Molecular imprinting technology (MIT)

Molecular imprinted polymer (MIP)

N,N-dimethyl formamide (DMF),

Non-imprinted polymer (NIP)

N-Methylmorpholine N-oxide (NMMO),

polycaprolactone-triol (PCL-T)

Scanning electron microscopy (SEM)

transdermal drug delivery (TDD)

Ultra violet (UV)

Acknowledgment

The authors are grateful to Science and Research Branch of Islamic Azad University for all of their supports.

Declaration of Interests

The authors declare that there is not any conflict of interests.

References

1. Fishman MA, Scherer A, Topfer J, Kim PS. Limited access to on-label formulations of buprenorphine for chronic pain as compared with conventional opioids. Pain Medicine. 2020 May 1;21(5):1005-9.

2. Ritvo AD, Calcaterra SL, Ritvo JI. Using extended-release buprenorphine injection to discontinue sublingual buprenorphine: a case series. Journal of addiction medicine. 2021 May 1;15(3):252-4.

3. Ritvo AD, Calcaterra SL, Ritvo JI. Using extended release buprenorphine injection to discontinue sublingual buprenorphine: a case series. Journal of addiction medicine. 2021 May 1;15(3):252-4.

4. Eriksson A, Jeppesen S, Krebs L. Induction of labour in nulliparous women-quick or slow: a cohort study comparing slow-release vaginal insert with low-dose misoprostol oral tablets. BMC Pregnancy and Childbirth. 2020 Dec;20:1-8.

5. Behnia N, Azar PA, Shekarchi M, Tehrani MS, Adib N. Synthesis of a new molecular imprinted polymer for oxycodone opioid and its formulation for transdermal controlled drug delivery application: A joint experimental and quantum chemical study. ChemistrySelect. 2022 Oct 13;7(38):e202202553.

6. Lee HY, Kim HE, Jeong SH. One-pot synthesis of silane-modified hyaluronic acid hydrogels for effective antibacterial drug delivery via sol–gel stabilization. Colloids and Surfaces B: Biointerfaces. 2019 Feb 1;174:308-15.

7. Lee HY, Kim HE, Jeong SH. One-pot synthesis of silane-modified hyaluronic acid hydrogels for effective antibacterial drug delivery via sol–gel stabilization. Colloids and Surfaces B: Biointerfaces. 2019 Feb 1;174:308-15.

8. Ganjavi F, Ansari M, Kazemipour M, Zeidabadinejad L. Computer- aided design and synthesis of a highly selective molecularly imprinted polymer for the extraction and determination of buprenorphine in biological fluids. Journal of Separation Science. 2017 Aug;40(15):3175-82.

9. Gokulakrishnan K, Prakasam T. Preparation and evaluation of molecularly imprinted polymer liquid chromatography column for the separation of ephedrine enantiomers. Arabian Journal of Chemistry. 2016 Sep 1;9:S528-36.

10. a) Panahi Y, Motaharian A, Hosseini MR, Mehrpour O. High sensitive and selective nano-molecularly imprinted polymer based electrochemical sensor for midazolam drug detection in pharmaceutical formulation and human urine samples. Sensors and Actuators B: Chemical. 2018 Nov 10;273:1579-86.; b) Siadati A. A theoretical study on the possibility of

functionalization of C20 fullerene via its Diels-Alder reaction with 1, 3-butadiene. Letters in Organic Chemistry. 2016 Jan 1;13(1):2-6.

11. Rezaei M, Rajabi HR, Rafiee Z. Selective and rapid extraction of piroxicam from water and plasma samples using magnetic imprinted polymeric nanosorbent: Synthesis, characterization and application. Colloids and Surfaces A: Physicochemical and Engineering Aspects. 2020 Feb 5;586:124253.

12. Cieplak M, Kutner W. Artificial biosensors: How can molecular imprinting mimic biorecognition?. Trends in biotechnology. 2016 Nov 1;34(11):922-41.

13. Wang Z, Duan Y, Duan Y. Application of polydopamine in tumor targeted drug delivery system and its drug release behavior. Journal of Controlled Release. 2018 Nov 28;290:56-74.

14. M.A. Tryfonidou, G. de Vries, W.E. Hennink, L.B. Creemers, Adv. Drug Del. Rev., 160, 170 (2020).

15. Jun XU, WANG XY, GUO WZ. The cytochrome P450 superfamily: Key players in plant development and defense. Journal of Integrative Agriculture. 2015 Sep 1;14(9):1673-86.

16. Karameta E, Gourgouliani N, Kouvari-Gaglia D, Litsi-Mizan V, Halle S, Meiri S, Sfenthourakis S, Pafilis P. Environment shapes the digestive performance in a Mediterranean lizard. Biological Journal of the Linnean Society. 2017 Aug 1;121(4):883-93.

17. a) Siadati S, Amin M, Meghdad M, Beheshti A. Development and validation of a short runtime method for separation of trace amounts of 4-aminophenol, phenol, 3-nitrosalicylic acid and mesalamine by using HPLC system. Current Chemistry Letters. 2021;10(3):151-60.; b) Beheshti A, Kamalzadeha Z, Haj-Maleka M, Payaba M, Rezvanfar M, Siadati S. Development and validation of a reversed-phase HPLC method for determination of assay content of Teriflunomide by the aid of BOMD simulations. Current Chemistry Letters. 2021;10(3):281-94.

18. A.C. Alves, I.I. Ramos, C. Nunes, L.M. Magalhães, H. Sklenářová, M.A. Segundo, S. Reis, *Talanta*, 146, 369 (2016).

19. Seo JE, Kim S, Kim BH. In vitro skin absorption tests of three types of parabens using a Franz diffusion cell. Journal of exposure science & environmental epidemiology. 2017 May;27(3):320-5.

20. a) Dadras A, Rezvanfar MA, Beheshti A, Naeimi SS, Siadati SA. An urgent industrial scheme both for total synthesis, and for pharmaceutical analytical analysis of umifenovir as an anti-viral API for treatment of COVID-19. Combinatorial Chemistry & High Throughput Screening. 2022 Apr 1;25(5):838-46; b) Siadati SA, Davoudi S, Soheilizad M, Firoozpour L, Payab M, Bagherpour S, Kolivand S. The synthesis and the mechanism of a five-membered

ring formation between an isothiocyanate and an amide leading to the yield of Enzalutamide anticancer API; a joint experimental and theoretical study. Journal of Molecular Structure. 2023 May 15;1280:135057.

21. a) Siadati SA, Payab M, Beheshti A. Development of a reversed-phase HPLC method for determination of related impurities of Lenalidomide. Chemical Review and Letters. 2020 Apr 1;3(2):61-4; b) Siadati SA, Soheilizad M, Firoozpour L, Samadi M, Payab M, Bagherpour S, Mousavi SM. An Industrial Approach to Production of Tofacitinib Citrate (TFC) as an Anti-COVID-19 Agent: A Joint Experimental and Theoretical Study. Journal of Chemistry. 2022 Dec 9;2022.

22. Trinovita E, Saputri FC, Mun'im A. Enrichment of the gamma oryzanol level from rice bran by addition of inorganic salts on ionic liquid 1-butyl-3-methylimidazolium hexafluorophosphate ([BMIM] PF6) extraction. Journal of Young Pharmacists. 2017;9(4):555.

23. Kellum JA. Disorders of acid-base balance. Critical care medicine. 2007 Nov 1;35(11):2630-6.

24. Han L, Tang C, Yin C. pH-responsive core–shell structured nanoparticles for triple-stage targeted delivery of doxorubicin to tumors. ACS Applied Materials & Interfaces. 2016 Sep 14;8(36):23498-508.